UDK 546.654:547.458.8
Original scientific article/Izvirni znanstveni članek

ISSN 1580-2949
Mater. Tehnol.

SYNTHESIS AND CHARACTERIZATION STUDIES OF CMC/NCC NANO COMPOSITES DERIVED FROM TEXTILE WASTE FOR THE ADSORPTION OF LANTHANUM IONS FROM AQUEOUS SOLUTIONS

SINTEZA IN KARAKTERIZACIJA CMC/NCC NANOKOMPOZITOV IZDELANIH IZ TEKSTILNIH ODPADKOV ZA ADSORPCIJO LANTANOVIH IONOV IZ VODNIH RAZTOPIN

Hasan Türkmen[1,2], Sabriye Yuşan[1], Cem Gök[3,4]

[1]Ege University, Institute of Nuclear Sciences, Bornova, 35100, Izmir, Turkey
[2]Pamukkale University, Faculty of Technology, Metallurgical and Materials Engineering, Denizli Turkey
[3]Izmir Bakırcay University, Faculty of Engineering and Architecture, Department of Biomedical Engineering, Menemen,35665, İzmir Turkey
[4]Izmir Bakırcay University, Biomedical Technologies Design Application and Research Center, Izmir, 35665, Türkiye

Prejem rokopisa – received: 2025-05-05; sprejem za objavo – accepted for publication: 2025-06-15

doi:10.17222/mit.2025.1446

This study investigated the adsorption efficiency of lanthanum (La) ions, a rare-earth element, using nanocrystalline cellulose (NCC)-reinforced carboxymethyl cellulose (CMC) biopolymers synthesized from textile waste. Microcrystalline cellulose (MCC) was derived via acid hydrolysis, followed by NCC synthesis through basic reaction. The characterization was performed using FT-IR, SEM, XPS and XRD analyses. Key adsorption parameters, including pH, initial concentration, agitation time, and temperature, were optimized. The adsorption process of La(III) ions onto the CMC/NCC nanocomposite follows the Langmuir isotherm model with a high adsorption capacity of 38.13 mg/g, indicating monolayer adsorption, while thermodynamic analysis reveals the process is endothermic, spontaneous at higher temperatures, and predominantly governed by physicochemical interactions. The CMC-NCC biopolymer presents an economical, effective, and eco-friendly alternative for lanthanum removal from aqueous solutions.

Keywords: Lanthanum, biosorption, nanocellulose, nanocomposite, rare earth elements

V članku avtorji predstavljajo študijo učinkovitosti adsorpcije redko-zemeljskega elementa lantana (La) z uporabo biopolimera na osnovi nanokristalinične celuloze (NCC), ojačane s karboksimetilno celulozo (CMC), sintetiziranega iz tekstilnega odpada. Mikrokristalinično celulozo (MCC) so izdelali s kislinsko hidrolizo, kateri je sledila NCC sinteza z osnovno reakcijo. Karakterizacijo biopolimera so avtorji izvedli z FT-IR, SEM, XPS in XRD analizami. Optimizirali so ključne adsorpcijske parametre in sicer: pH, začetno koncentracijo, čas in temperaturo obdelave. Adsorpcijski proces La(III) ionov na CMC/NCC nanokompozitu poteka v skladu z Langmuirjevim izotermnim modelom z veliko adsorpcijsko kapaciteto 38,13 mg/g. Avtorji ugotavljajo, da je vzrok za to adsorpcija po posameznih plasteh (angl.: monolayer adsorption). Termodinamične analize so pokazale, da je proces endotermen, spontan pri višjih temperaturah in ga prednostno obvladujejo fizikalno kemijske interakcije. CMC-NCC biopolimer predstavlja ekonomsko, učinkovito in okolju prijazno rešitev za odstranitev lantanovih ionov iz vodnih raztopin.

Ključne besede: lantan, biosorpcija, nanoceluloza, nanocompozit, redkozemeljski elementi

1 INTRODUCTION

The environmental impacts of textile waste are significant, contributing to sustainability challenges globally. The textile industry is one of the largest polluters, with millions of tons of waste generated annually. This waste often ends up in landfills, where it can take decades to decompose, releasing harmful substances into the soil and water systems [6]. Furthermore, the production of textiles is resource-intensive, consuming vast amounts of water and energy, and contributing to greenhouse-gas emissions.[4] The challenge of managing textile waste is compounded by the complexity of materials used in garments, which often include synthetic fibers that are not biodegradable.[4] Effective management strategies are crucial for reducing the environmental footprint of the textile industry.

Recycling textile waste presents a potential solution, transforming waste into valuable products. Innovations in recycling technologies can convert discarded textiles into new fibers or materials, thereby reducing the demand for virgin resources and minimizing waste 4. For instance, cellulose-based materials derived from textile waste can be repurposed into biocomposites or other sustainable products.[5] The potential for recycling is not only environmentally beneficial but also economically advantageous, as it can create new markets and job opportunities in the recycling sector.[6]

*Corresponding author's e-mail:
hasanturkmen@pau.edu.tr (Hasan Türkmen)

Cellulose-based materials, particularly carboxymethyl cellulose (CMC) and nanocrystalline cellulose (NCC), are gaining attention because of their structural properties and sustainability. CMC is known for its high solubility in water and ability to form gels, making it suitable for various applications, including food and pharmaceuticals.[7] NCC, on the other hand, exhibits a remarkable mechanical strength and a high surface area, which enhances its functionality in composite materials.[5] Both materials are biodegradable and derived from renewable resources, aligning with the principles of sustainability.[7] The incorporation of CMC and NCC into nanocomposites can significantly improve their mechanical properties and ion-adsorption capabilities, making them ideal for applications in environmental remediation.[5]

The economic and technological importance of rare-earth elements (REEs), particularly lanthanum, cannot be overstated. Lanthanum is utilized in various industrial applications, including catalysts, electronics, and magnetic materials.[1] The recovery of lanthanum from aqueous solutions is critical, as it not only supports the sustainability of REE supply chains but also mitigates the environmental pollution associated with mining activities.[3] The effectiveness of adsorption technology for recovering lanthanum ions from wastewater is particularly promising. Adsorption is an environmentally friendly and cost-effective method, utilizing various adsorbent materials to selectively remove the lanthanum ions from solutions.[2] This technology can significantly reduce the environmental impact of textile waste by enabling the recovery of valuable materials from effluents generated during textile processing.

The innovative aspect of this study lies in the first-time application of CMC/NCC nanocomposites derived from textile waste for lanthanum adsorption. This approach not only addresses the issue of textile waste but also contributes to the recovery of critical materials, aligning with both environmental and economic goals.[5] The findings of this study could pave the way for new sustainable practices in the textile industry, promoting a circular economy where waste is minimized, and resources are reused effectively.

In conclusion, the environmental impacts of textile waste and the challenges in managing it highlight the urgent need for innovative solutions. The potential for recycling textile waste into valuable products, particularly using cellulose-based materials, presents a sustainable pathway forward. Additionally, the economic and technological significance of REEs, coupled with effective adsorption technologies, underscores the importance of integrating waste-management strategies with resource-recovery efforts.

2 EXPERIMENTAL

2.1 Reagents and materials

The textile waste used for the synthesis of the reinforced NCC phase was sourced from local companies. The CMC utilized in the matrix phase was obtained in its Na-CMC form from Merck. Lanthanum stock standard solutions were prepared by dissolving an appropriate amount of lanthanum nitrate hexahydrate ($(La(NO_3)_3{\cdot}6H_2O)$ (Merck)) in deionized water. All reagents employed in this study were of analytical reagent (AR) grade. The pH of the solutions was regulated using dilute sodium hydroxide (NaOH) and hydrochloric acid (HCl) solutions.

2.2 Instrumentation Specifications

The properties of CMC/NCC samples were investigated using several analytical techniques, including scanning electron microscopy (SEM, Coxem EM-30), X-ray diffraction (XRD, Thermo Scientific ARL K-Alpha), X-ray photoelectron spectroscopy (XPS, Thermo Scientific Al K-Alpha), Fourier transform infrared spectroscopy (FTIR, PerkinElmer Spectrum Two).

Lanthanum concentrations in the solutions were analyzed using a Perkin-Elmer Optima 2000 DV inductively coupled plasma optical emission spectrometer (ICP-OES). The solution pH was adjusted with the help of a Hanna Instruments Model 8521 pH meter. Solution mixing was performed in a thermostatically controlled water bath shaker (GFL-1083 model).

2.3 Preparation of CMC/NCC

2.3.1 The Extraction of NCC

Nanocrystalline cellulose (NCC) was synthesized from cotton-based textile waste using a combined acid hydrolysis and alkaline dissolution method, offering a sustainable approach to material production. The process began with the conversion of textile waste into microcrystalline cellulose (MCC) through acid hydrolysis. Textile waste was treated with 1M HCl at 80 °C for 6 h to dissolve amorphous regions and remove impurities like lignin and hemicellulose, resulting in MCC with a crystalline index of approximately 70 %.[8,12] The hydrolyzed material was filtered, extensively washed with deionized water, and dried.

To transform MCC into NCC, the cellulose was dispersed in a NaOH/urea solution optimized at 7 % NaOH and 12 % urea concentrations.[10] This system enhanced cellulose solubility and served as an eco-friendly alternative.[11] The mixture was subjected to freezing at –18 °C, followed by thawing and centrifugation to isolate NCC. The NaOH and urea facilitated molecular-level dissolution by forming new hydrogen bonds between the cellulose chains, while precise temperature control preserved the cellulose structure.[12]

The resulting NCC displayed nanoscale structures with enhanced mechanical and functional properties, highlighting its potential for various industrial applications and contributing to sustainable material production.[9]

2.3.2 Preparation of CMC–NCC Nanocomposite Films

The preparation of a carboxymethyl cellulose (CMC) matrix phase involves a series of well-defined steps that ensure the formation of a stable and functional hydrogel. Initially, 3 g of CMC powder is dissolved in 100 mL of distilled water, which is then subjected to continuous stirring at 65 °C for 4 h. This heating process is crucial as it facilitates the dissolution of CMC, leading to a transparent solution, which is indicative of complete dissolution and uniformity in the polymer matrix.[13,17] The transparency of the solution is attributed to the hydrophilic nature of the CMC, which allows for effective hydrogen bonding and interaction with water molecules, enhancing its solubility.[17]

Following the dissolution, crosslinking is achieved by incorporating 2 g of citric acid into the solution. Citric acid acts as a crosslinking agent through an esterification reaction with the hydroxyl groups of CMC, forming a network that enhances the thermal and chemical stability of the resulting hydrogel.[13,21] The curing process at 65 °C for 24 h allows for the complete formation of ester bonds, which are critical for the mechanical integrity and durability of the hydrogel.[18,20] This crosslinking mechanism is essential for creating a robust structure that can withstand various environmental conditions, thereby improving the hydrogel's applicability in biomedical and agricultural fields.[15]

The incorporation of nanocrystalline cellulose (NCC) into the CMC matrix is aimed at enhancing the mechanical properties of the hydrogel. By adding NCC in varying compositions (10 mL/100 mL), the mixture is stirred for approximately 2 h to achieve homogeneity. The addition of NCC not only improves the mechanical strength of the CMC films but also contributes to their thermal stability, as evidenced by studies indicating that nanocellulose reinforcement leads to enhanced thermal degradation temperatures.[16,22] The resulting CMC/NCC films are then cast in petri dishes and allowed to dry at room temperature, facilitating solvent evaporation and the consolidation of the hydrogel structure.[23]

After drying, the films undergo a washing process with deionized water to remove any unreacted materials or byproducts, ensuring the purity of the final product.[13,18] The films are then filtered and stored at +4 °C to maintain their integrity for future applications. This storage condition is essential for preserving the physical and chemical properties of the hydrogel, which can be sensitive to temperature fluctuations.[14,19] Overall, the methodology described for preparing the CMC/NCC films highlights the importance of each step in achieving a high-quality hydrogel suitable for various applications, particularly in drug delivery and tissue engineering.[24]

2.4 Characterization of CMC/NCC

Analyzes for the structural characterization of CMC/NCC biyonanocomposites were carried out by Ege University Nuclear Science Institute, Ege University Central Research Laboratory (MATAL), Pamukkale University Metallurgical and Materials Engineering, Pamukkale University Advanced Technology Research Laboratory (İLTAM)

To characterize the bionanocomposites, various analytical techniques were employed: X-ray Diffraction (XRD) was used to examine the crystalline structure and phases; Scanning Electron Microscopy (SEM) provided information on particle morphology and size; Fourier Transform Infrared Spectroscopy (FTIR) identified functional group interactions and bonding properties; X-ray Photoelectron Spectroscopy (XPS) analyzed surface chemistry; and surface area analysis measured the material's porosity and adsorption capacity.

2.5 La (III) ions adsorption experiments

The adsorption experiments for La (III) ions were conducted using a GFL-1083 thermostat batch system with a water-bath shaker. CMC/NCC was employed as the adsorbent, and the study was performed at varying temperatures, contact times, La (III) ion concentrations, and pH values using Lanthanum Nitrate Hexahydrate ($La(NO_3)_3{\cdot}6H_2O$) solutions. The pH of the solutions was adjusted using diluted sodium hydroxide (NaOH) and hydrochloric acid (HCl) solutions. The residual concentration of La (III) ions in the solution after adsorption was measured using a Perkin Elmer Optima 2000 DV ICP-OES instrument. Each experimental condition was tested with three parallel samples, and the average values of the results were utilized for analysis.

The influence of various parameters on the adsorption process, including pH, initial concentration, volume-to-mass ratio (*V*/*m*), contact time, temperature, and the presence of different ions, was systematically studied. Key metrics such as the quantity of adsorbed La (III) ions, dispersion coefficient (K_d), and adsorption percentage (q_e) were calculated and analyzed to evaluate the process efficiency.

The influence of pH, initial ion concentration, volume-to-mass ratio (*V*/*m*), temperature, and the varying concentrations of foreign ions on the adsorption process was systematically examined. Essential parameters such as the quantity of adsorbed La(III) (q_e, mg/g), the distribution coefficient (K_d, mL/g), and the adsorption efficiency (%) were evaluated. The required calculations were conducted using the equations outlined below:

$$q_e = \frac{(C_0 - C_e)V}{W} \text{ (mg/g)} \quad (1)$$

$$K_d = \frac{(C_0 - C_e)V}{C_e W} \text{ (mL/g)} \quad (2)$$

$$\% \text{ of Adsorption} = \frac{C_0 - C_e}{C_0} \quad (3)$$

where C_0 and C_e represent the initial and equilibrium concentrations of metal ions (mg/L), respectively, V is the volume of the solution (L), and m is the mass of the adsorbent (g).

3 RESULTS AND DISCUSSION

3.1 Structural and morphological properties

The XRD patterns were analyzed to identify the phases present when CMC/NCC was used as an adsorbent in powder form. The XRD spectrum of the material, measured at 2θ angles, is presented in **Figure 1**.

The analysis of X-ray diffraction (XRD) patterns is crucial for identifying the crystalline and amorphous phases present in materials such as carboxymethyl cellulose (CMC) and nanocrystalline cellulose (NCC). In the case of NCC, the XRD spectrum typically reveals characteristic peaks at 2θ angles of approximately 15.2°, 16.2°, 22.8°, and 34.7°, which correspond to the cellulose type-I diffraction planes ($1\bar{1}0$, 110, 200, and 004) (Lin et al., 2018; Trilokesh & Uppuluri, 2019). These

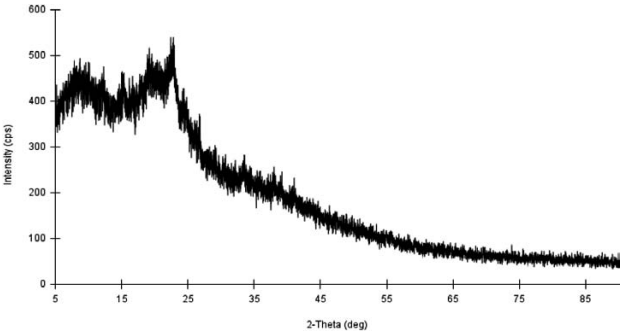

Figure 1: X-Ray Diffraction (XRD) pattern of CMC/NCC bionanocomposites

peaks indicate a high degree of crystallinity, which is essential for the mechanical properties and biocompatibility of NCC, making it suitable for various applications in materials science.[25]

The internal structure of the CMC/NCC nanocomposite was examined by scanning electron microscopy, and images were obtained **Figure 2**. SEM images reveal the highly ordered, polyhedral structure of nanocrystalline cellulose (NCC), which results from the crystalline regions formed during partial cellulose hydro-

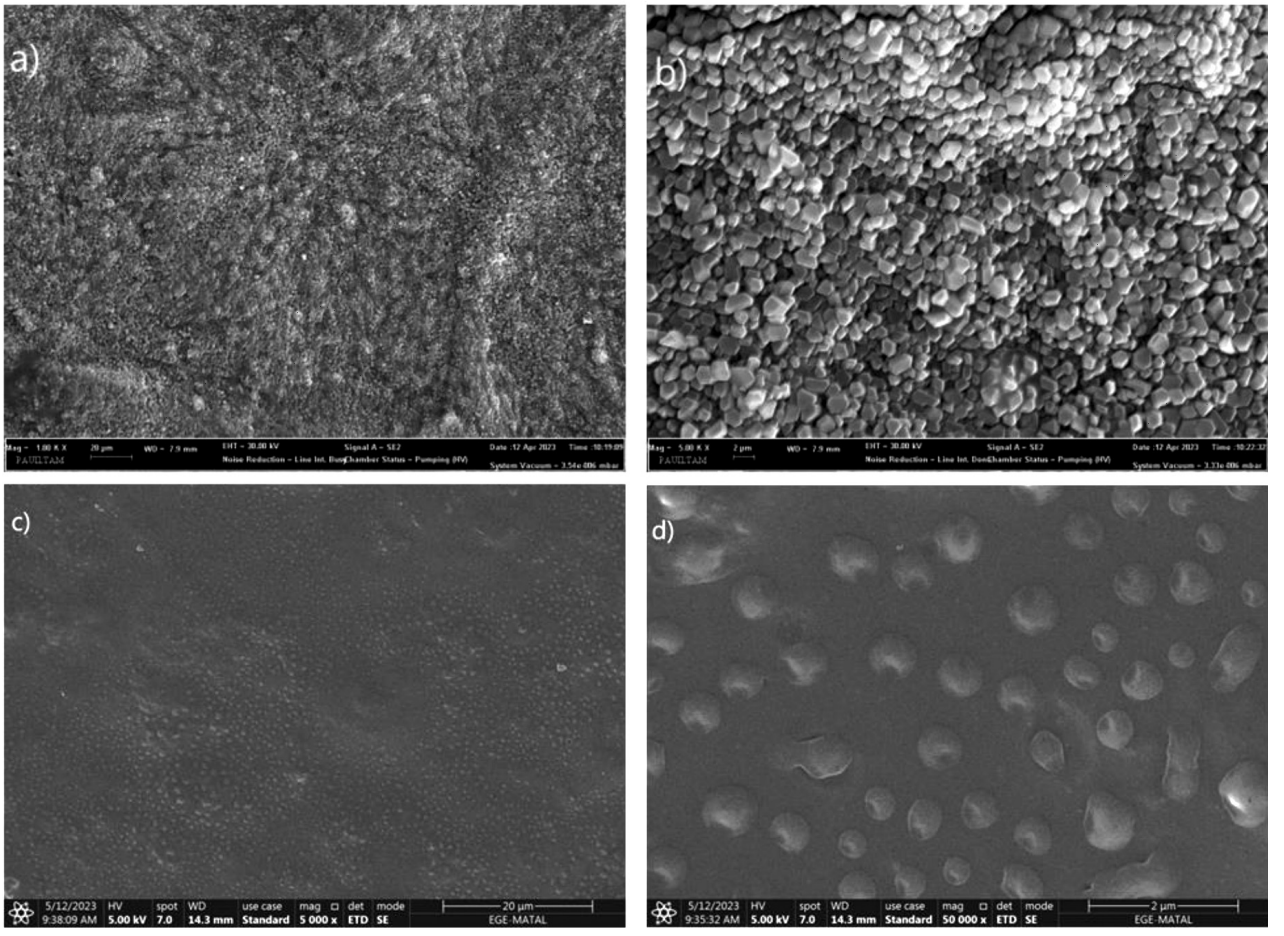

Figure 2: Scanning Electron Microscope (SEM) image of a) NCC particles 1.000x, b) NCC particles 5.000x, c) CMC/NCC bionanocomposites 5.000x d) CMC/NCC bionanocomposites 50.000 x

lysis.[35] This structural organization enhances the mechanical properties, including hardness, strength, and chemical resistance. The incorporation of NCC influences the composite's overall performance by improving the load transfer within the polymer matrix, thereby increasing mechanical and thermal properties.[29,33,34] NCC's high aspect ratio and surface area facilitate strong interactions with the polymer matrix, improving stability under various conditions.[32] SEM analysis highlights the importance of NCC's crystalline nature and its role in optimizing nanocomposite functionality. The structural and morphological characteristics observed align with studies emphasizing NCC's critical contribution to the enhanced performance of nanocomposite materials.[30,31,35]

FTIR spectroscopy was employed to analyze the vibrational modes of CMC/NCC bionanocomposites, revealing crucial functional groups and their interactions. The spectrum displayed a broad OH stretching band at 3393 cm^{-1}, indicating hydroxyl groups that enhance water retention and structural stability.[26] Peaks at 2927 cm^{-1} (C-H stretching) and 1720 cm^{-1} (C=O stretching) signify hydrocarbon and carbonyl groups, which serve as important sites for ion adsorption.[27] Carboxylate groups were identified at 1408 cm^{-1} and 1224 cm^{-1}, further improving the ion binding capacity. Additionally, vibrations between 676 cm^{-1} and 812 cm^{-1} reflect structural features like C-H and C-O-C bonds, highlighting the composite's functional versatility. Overall, the FTIR analysis underscores the significance of these functional groups in enhancing the material's properties for various applications, including environmental remediation.[28]

Dynamic light scattering (DLS) analysis of the nanocrystalline cellulose (NCC) indicates a narrow size distribution of 300–600 nm, enhancing its surface area for adsorption interactions[41] The high crystallinity and transformation from cellulose I to cellulose II increases the internal surface area, boosting adsorption capabilities.[37] NCC's mechanical properties, reinforced through hydrogen bonding, create a rigid network within matrices like biodegradable polymers, enhancing mechanical

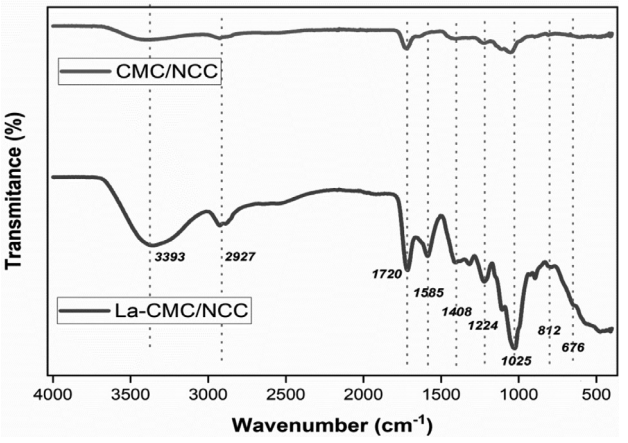

Figure 3: FTIR spectroscopy spectrum of CMC/NCC

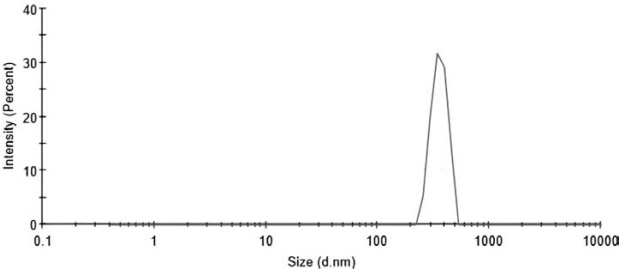

Figure 4: Dynamic light scattering (DLS) analysis of nanocrystalline cellulose (NCC)

strength and adsorption efficiency.[42,38] NCC's biodegradability and renewability make it ideal for environmental remediation, especially for removing heavy metals and rare earth elements.[39,43] Its high surface area and hydroxyl groups facilitate complex formation with ions, making NCC effective for selective adsorption and resource recovery from effluents.[40,44,36]

The binding energies of La 3d are critical for understanding the chemical bonding characteristics of lanthanum. The La 3d5/2 and La 3d3/2 double peaks are observed in the ranges of 835–840 eV and 849–855 eV, respectively. These binding energies confirm that La^{3+} ions are chemically adsorbed on the surface. This ionic form of lanthanum exhibits different chemical interactions on various surfaces and environments. Specifically, the interactions of La^{3+} ions on surfaces are associated with chemical bonding processes. For instance, the adsorption energy of La^{3+} ions on TiO_2 surfaces has been calculated as –858.30 kJ/mol, indicating the formation of new chemical bonds.[47] This suggests that La^{3+} ions form strong chemical bonds with other surface components, causing changes in the energy levels of these bonds. Moreover, the adsorption behavior of La^{3+} ions is driven by Coulomb interactions.[48] In this context, the interactions of La^{3+} ions on the surface significantly influence their interactions with other surface components. The binding energies of La^{3+} ions play an essential role in understanding chemical bonding processes on surfaces. For example, changes in the O1s spectrum of La^{3+} ions can be used to elucidate the chemical bonding processes on

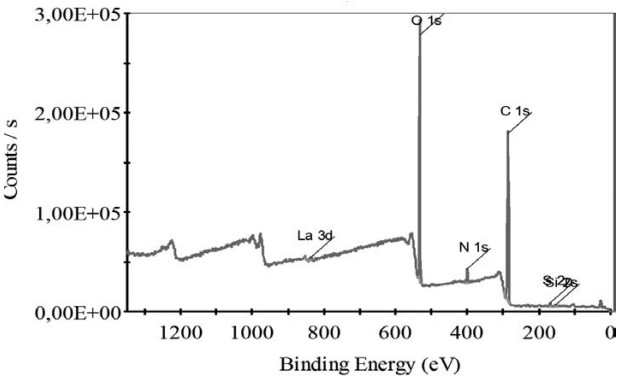

Figure 5: X-ray Photo Emission Spectroscopy (XPS) spectra of nanocrystalline cellulose (NCC)

surfaces. In compounds such as LaOCl, the O 1s peaks can distinguish between O^{2-} ions in the crystal lattice and adsorbed oxygen species.[49] Such analyses are crucial for gaining a deeper understanding of the chemical bonding processes involving La^{3+} ions on surfaces.

3.2 Adsorption studies

3.2.1 pH effect

Maintaining the concentration of La (III) ions at 25 mg/L, a range of pH values from 2 to 8 was tested to identify the optimal conditions for effective adsorption. However, precipitation occurred at pH levels above 6, resulting in unreliable data at these higher pH values, which were therefore excluded from further analysis.[45]

As illustrated in **Figure 6**, the optimal adsorption efficiency was observed at pH 5, achieving a yield of 78.29 %.

3.2.2 La concentration effect

To evaluate the effect of initial La (III) ion concentration on adsorption, solutions with concentrations of (10, 25, 50, 75, 100, 125 and 150) mg/L were prepared. Each solution was adjusted to a volume of 25 mL at pH 5, and 0.0025 g of CMC/NCC was added. Adsorption experiments were conducted at room temperature (25 °C) for 15 minutes using a water bath shaker. The adsorption capacities of the CMC/NCC for La (III) ions are presented in **Figure 6**.

It is seen that 0.0025 g CMC/NCC has the highest adsorption yield 79.06 % of 25 mg/L according to the initial test constants.

Figure 7: Adsorption capacities of the different concentrations effect. (*c*: 25, 50, 75, 100, 125, 150 mg/L, *m*: 0.0025 g, *V*: 25 mL, pH: 5, *t*: 120 min, *T*: 25 °C)

3.2.3 Time effect

The effect of contact time on the adsorption efficiency of the La (III) ions using CMC/NCC as an adsorbent was investigated over 10 min to 240 min. The adsorption results as a function of contact time are illustrated in **Figure 8**. The highest adsorption efficiency

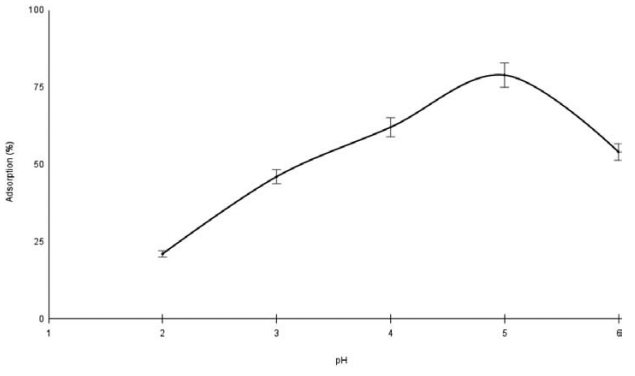

Figure 6: Adsorption capacities of the different pH values effect. (*c*: 25 mg/L, m: 0.0025 g, *V*: 25 mL, pH:2,3,4,5,6, *t*: 120 min, *T*: 25 °C) pH: 7,8,9 has no value cause of precipitation of Lanthanum

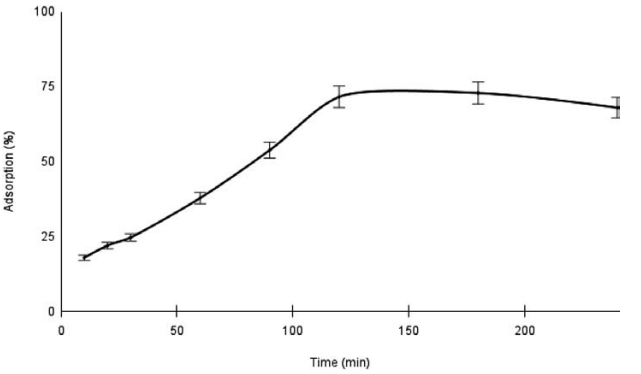

Figure 8: Adsorption capacities of the time effect. (*c*: 25 mg/L, *m*: 0.0025 g, *V*: 25 mL, pH:5, *t*: 10, 20, 30, 60, 90, 120, 180 min, *T*: 25 °C)

was observed at 120 min. This trend can be attributed to the gradual occupation of the available active sites on the adsorbent surface during the initial phase, leading to effective binding of La (III) ions. However, beyond 120 min, irregular desorption of particles from the adsorbent surface into the solution was observed. This phenomenon may be caused by competing forces that destabilize the adsorbed particles, which initially adhered due to strong interactions. Over time, particle interactions stabilize due to consistent magnetic polarities, which enhance the adsorption process's efficiency. From an economic and practical perspective, 120 min was identified as the optimal contact time, balancing maximum adsorption efficiency and operational feasibility.

3.3 Adsorption equilibrium models

Adsorption, defined as the accumulation of substances on a surface, serves as a fundamental mechanism for mass transport in various systems. This process can be described through mathematical modeling using experimental data ratios. When the adsorption of dissolved metal ions onto the adsorbent surface reaches equilibrium, these ratios are applied to develop the isotherm models. Adsorption is typically modeled as an isotherm, which represents the relationship between the amount of adsorbed metal ions and their equilibrium concentration at a constant temperature. Among the numerous isotherms, Langmuir, Freundlich, and Dubinin-Radushkevich (D-R) models are widely utilized to analyze adsorption equilibrium data. In this study, these three isotherms were employed to evaluate the adsorption behavior of the La (III) ions on CMC/NCC. The correlation constants derived from each isotherm model are presented in Table 1. Adsorption experiments were conducted using La (III) solutions with concentrations ranging from 25 mg/L to 150 mg/L and 25 mg of CMC/NCC under optimal conditions: 25 °C, 5 mL solution volume, pH 5, and 120 min of contact time.

In an adsorption process that aligns with the Langmuir model, the adsorbate (La (III)) is uniformly distributed across the surface of the adsorbent (CMC/NCC), in-

dicating a monolayer adsorption mechanism. The equilibrium condition in the Langmuir isotherm is defined by the dynamic balance between the rate of ions desorbing from the adsorbent surface into the solution and the rate of ions adsorbing from the solution onto the adsorbent surface. This equilibrium ensures a consistent and predictable adsorption behavior, characteristic of the Langmuir model.

The Langmuir equation is represented as follows:

$$\frac{C_e}{q_e} = \frac{1}{Q_0 b_L} + \frac{C_e}{Q_0} \quad (4)$$

C_e: Equilibrium concentration of ions.
q_e: Quantity of adsorbed ions at the equilibrium condition.
Q_o: Langmuir equilibrium constant
b_L: Langmuir constant (mean partial concentration)
Q_0 and b_L were calculated from the slope and intercept of linear plots of $C_e/q_e - C_e$.

Freundlich proposed that adsorption occurs on heterogeneous surfaces in multiple layers, with the adsorption intensity varying across the surface. The adsorption distribution follows an exponential trend, and the corresponding equation is:

$$\log q_e = \log K_F + \frac{1}{n_f} \log C_e \quad (5)$$

K_F: Adsorption capacity (mg/g)
n_f: Adsorption intensity (dimensionless)

Dubinin and Radushkevich postulated that the adsorption occurs primarily within the pores and micropore volumes of the adsorbent surface, where the adsorbed particles undergo a loss of energy. The equation for the D-R model is:

$$\ln X = (-\beta\varepsilon^2) \ln X_m \quad (6)$$

X: Adsorbed solution of 1-gram adsorbent (mmol/g)
X_m: Maximum amount of adsorbed particles of 1-gram adsorbent (mmol/g)
β: Constant related to energy (mol/K)^2
ε: Polanyi potential

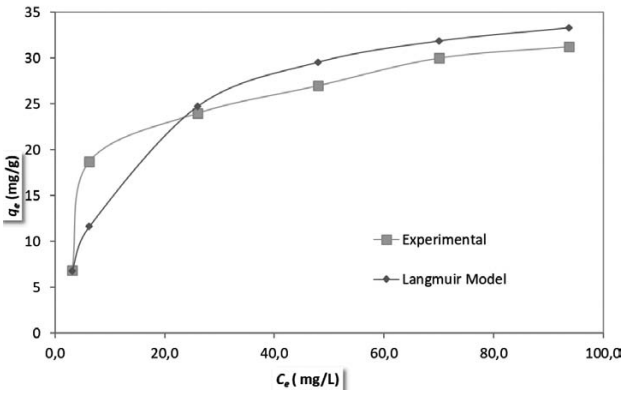

Figure 9: Experimental and Langmuir isotherms models for La (III) adsorption on CMC/NCC

$$\varepsilon = RT \ln\left(\frac{1}{1+C_e}\right) \quad (7)$$

Table 1: Isotherm constants of models for lanthanum adsorption onto CMC/NCC

Isotherm models	Parameters	Linearized isotherm
Langmuir	Q_o (mg/g)	38.13
	b_L (L/mg)	0.0697
	R^2	0.9722
Freundlich	K_F (mg/g)	6.390
	n_F	2.676
	R^2	0.8447
Dubinin–Radushkevich	X_m (mg/g)	29.69
	β (mol/kJ)^2	$3.075 \cdot 10^{-6}$
	E (kJ/mol)	0.4032
	R^2	0.9466

The adsorption equilibrium data were analyzed using Langmuir, Freundlich, and Dubinin–Radushkevich (D–R) isotherm models to evaluate the adsorption behavior of La(III) ions onto the CMC/NCC nanocomposite. The correlation coefficients (R^2) derived from each model indicate that the Langmuir isotherm provides the best fit to the experimental data, with an R^2 value of 0.9722. This suggests that the adsorption process predominantly follows a monolayer adsorption mechanism, where the La(III) ions uniformly occupy specific homogeneous sites on the adsorbent surface. The Langmuir constants Q_0 and b_L, representing the maximum adsorption capacity and the binding strength, were calculated as 38.13 mg/g and 0.0697 L/mg, respectively. These values highlight the high efficiency of the CMC/NCC nanocomposite in adsorbing La(III) ions under optimal conditions. In contrast, the Freundlich isotherm model, which accounts for adsorption on heterogeneous surfaces and multilayer adsorption, yielded an R^2 value of 0.8447. The Freundlich constant K_F, representing the adsorption capacity, was determined as 6.390 mg/g, with $n_F = 2.676$, indicating favorable adsorption. However, the lower R^2 value suggests that the surface heterogeneity and multilayer adsorption effects are not predominant for this system. The D–R isotherm model, which describes adsorption into the pores of the adsorbent, produced an R^2 value of 0.9466. The mean free energy was calculated as 0.4032 kJ/mol, indicating that the adsorption process is predominantly physical, as $E < 8$ kJ/mol is characteristic of physisorption. Overall, the analysis confirms that the Langmuir model is the most suitable for describing the adsorption behavior of the La(III) ions onto the CMC/NCC nanocomposite. This finding underscores the monolayer adsorption nature of the process, with a high affinity for the adsorbent sites and efficient ion removal under the studied conditions. These results align with the thermodynamic evaluations and further validate the potential of CMC/NCC as an effective adsorbent for rare-earth ions in aqueous solutions.

3.4 Thermodynamic effect

In this study, the adsorption efficiency was evaluated within the temperature range 20–40 °C, and the corresponding thermodynamic parameters were determined. The thermodynamic parameters, including enthalpy change (ΔH^0), entropy change (ΔS^0), and Gibbs free energy change (ΔG^0), were calculated using the following equations:

$$\ln K_d = \frac{\Delta S^0}{R} - \frac{\Delta H^0}{RT} \quad (8)$$

$$\Delta G^0 = \Delta H^0 - T\Delta S^0 \quad (9)$$

The enthalpy change (ΔH^0, kJ/mol) and entropy change (ΔS^0, J/mol·K) were determined from the slope and intercept of the linear plot of lnKd versus 1/T (**Figure 12**). The Gibbs free energy change (ΔG^0) of adsorption was calculated using Equation (9).

The thermodynamic parameters for the adsorption of La (III) ions onto the CMC/NCC are presented in **Table 2**. The positive value of enthalpy (ΔH^0) confirms the endothermic nature of the adsorption process, indicating that the adsorption is influenced by the temperature. The ΔH^0 value, ranging between 20.9 kJ/mol and 80 kJ/mol, suggests that the adsorption mechanism involves both physical and chemical interactions, indicative of physicochemical adsorption.[22]

The Gibbs free energy change (ΔG^0) decreases with increasing temperature, as shown in **Table 2**, which signifies that the adsorption process becomes more spontaneous and thermodynamically favorable at higher temperatures. Furthermore, the positive value of entropy change (ΔS^0) highlights the increased randomness at the solid-liquid interface during adsorption and supports the stability of the adsorption process through complexation.[23]

Table 2: Thermodynamic parameters for La (III) adsorption on CMC/NCC

ΔH^0 (kJ/mol)	ΔS^0 (J/molK)	ΔG^0 (kJ/mol)				
–4,869	–160.63	293.15	298.15	303.15	313.15	323.15
		–0.4261	–2.306	0.1089	0.2336	0.3015

The thermodynamic parameters calculated in this study provide valuable insights into the adsorption process. The enthalpy change ΔH^0 was determined to be –4.869 kJ/mol, indicating that the adsorption is an exothermic process. This suggests that the adsorption releases heat, and the efficiency of the process may decrease with increasing temperature, as observed in the experimental data. The negative value of the entropy change indicates a reduction in the system disorder during the adsorption process, reflecting a more ordered arrangement of the adsorbed ions on the adsorbent surface. The Gibbs free energy change showed temperature dependence, with negative values at 20 °C and 25 °C, suggesting that the adsorption process is spontaneous at these temperatures. However, at higher temperatures (30 °C, 40 °C, and 50°C), ΔG^0 values became positive, indicating that the process is no longer spontaneous and may require an external energy input. This temperature dependency aligns with the exothermic nature of the adsorption, as exothermic processes typically favor lower temperatures. Overall, these results suggest that the adsorption process is thermodynamically favorable and efficient at lower temperatures, with maximum spontaneity observed around 20–25 °C. The negative entropy change implies a controlled and structured adsorption mechanism, likely driven by strong interactions between the adsorbent and the ions in solution. These findings are critical for optimizing operational conditions and enhancing the performance of the adsorption system in practical applications.

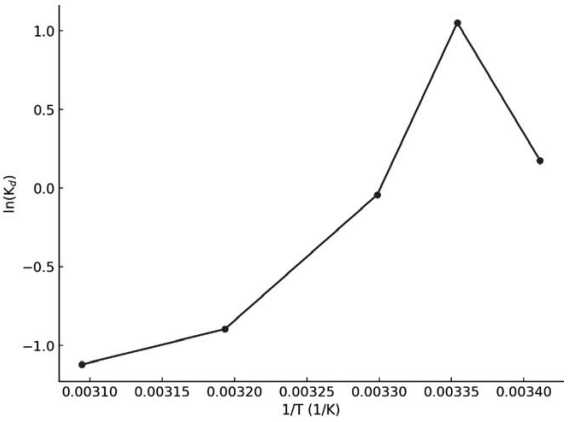

Figure 10: ln K_d – 1/T graph for La (III) adsorption on CMC/NCC

4 CONCLUSION

The CMC/NCC nanocomposite was synthesized through a partial reduction co-precipitation method, a straightforward, cost-effective, and environmentally sustainable approach for the adsorption of La (III) ions from aqueous solutions. The synthesized nanocomposite was extensively characterized using SEM, TEM, XRD, FTIR, XPS techniques. These analyses, combined with literature comparisons, confirmed the successful synthesis of CMC/NCC with the desired structural and magnetic properties. The adsorption of La(III) ions onto the CMC/NCC nanocomposite was found to follow the Langmuir isotherm model, indicating a monolayer adsorption mechanism on a homogeneous surface, with a maximum adsorption capacity of 38.13 mg/g. Thermodynamic analysis revealed that the process is endothermic and spontaneous at elevated temperatures, driven by physicochemical interactions, including ion exchange and complexation. These findings highlight the efficiency and potential of CMC/NCC nanocomposites as a sustainable and high-performance adsorbent for rare-earth ion removal, contributing to environmental remediation and resource-recovery efforts. These find-

ings suggest that CMC/NCC nanocomposite is an effective and promising adsorbent for the removal of La (III) ions from aqueous solutions, offering potential applications in environmental remediation.

Acknowledgements

The authors express their gratitude to the Scientific Research Council of Ege University, Turkey, for the financial support provided through research grant 24045. This study was also carried out within the scope of the project titled "Synthesis, characterization, and investigation of the use of nano-biocomposites in the recovery of rare earth elements," supported by the TÜBİTAK-2211-C National Doctoral Priority Areas Research Fellowship Program.

Declarations

Conflict of interest

The authors declare that there is no conflict of interest.

Data and code availability

Not Applicable

Supplementary information

Not Applicable

Ethical approval

Not Applicable

5 REFERENCES

[1] A. Fritz, T. Tarka, M. Mauter. Technoeconomic assessment of a sequential step-leaching process for rare earth element extraction from acid mine drainage precipitates. Acs Sustainable Chemistry & Engineering, 9 (**2021**) 28, 9308–9316. doi:10.1021/acssuschemeng.1c02069

[2] H. Gamal, W. Mohrez, A. Abdel-Kareem, H. Mashaal, H. El-Aziz, H. El-fatah, Leaching of rare earth elements from gibbsite-bearing shale of southwestern sinai, egypt using ammonium sulfate via ion exchange mechanism. Egyptian Journal of Chemistry, (**2023**). 0(0), 0-0. doi:10.21608/ejchem.2023.198156.7691

[3] D. Guyonnet, M. Planchon, A. Rollat, V. Escalon, J. Tuduri, N. Charles, … H. Fargier, Material flow analysis applied to rare earth elements in europe. Journal of Cleaner Production, 107 (**2015**), 215–228. doi:10.1016/j.jclepro.2015.04.123

[4] K. Immonen, S. Metsä-Kortelainen, J. Nurmio, A. Tribot, T. Turpeinen, A. Mikkelson, … H. Kangas, Recycling of 3d printable thermoplastic cellulose-composite. Sustainability, 14 (**2022**) 5, 2734. doi:10.3390/su14052734

[5] K. Immonen, P. Willberg-Keyriläinen, J. Ropponen, A. Nurmela, S. Metsä-Kortelainen, O. Kaukoniemi, … H. Kangas, Thermoplastic cellulose-based compound for additive manufacturing. Molecules, 26 (**2021**) 6, 1701. doi:10.3390/molecules26061701

[6] D. Mohan, Z. Teong, A. Bakir, M. Sajab, H. Kaco, Extending cellulose-based polymers application in additive manufacturing technology: a review of recent approaches. Polymers, 12 (**2020**) 9, 1876. doi:10.3390/polym12091876

[7] C. Valls, F. Pastor, M. Roncero, T. Vidal, P. Diaz, J. Martínez, … S. Valenzuela, Assessing the enzymatic effects of cellulases and lpmo in improving mechanical fibrillation of cotton linters. Biotechnology for Biofuels, 12 (**2019**) 1. doi:10.1186/s13068-019-1502-z

[8] R. Adawiyah, V. Suryanti, P. Pranoto, Preparation and characterization of microcrystalline cellulose from lembang (typha angustifolia l.). Journal of Physics Conference Series, 2190 (**2022**) 1, 012007. doi:10.1088/1742-6596/2190/1/012007

[9] A. Boondaeng, J. Keabpimai, P. Srichola, P. Vaithanomsat, C. Trakunjae, N. Niyomvong, Optimization of textile waste blends of cotton and pet by enzymatic hydrolysis with reusable chemical pretreatment. Polymers, 15 (**2023**) 8, 1964. doi:10.3390/polym15081964

[10] Q. Hu, Q. Yang, L. Zhang, T. Liebert, T. Heinze, The dissolution of cellulose in naoh-based aqueous system by two-step process. Cellulose, 18 (**2010**) 2, 237–245. doi:10.1007/s10570-010-9477-8

[11] Z. Karchangi, R. Behrooz, Preparation of microcrystalline cellulose using cotton yarn waste from the textile industry and evaluation of its characteristics. Bioresources, 18 (**2022**) 1, 1115–1127. doi:10.15376/biores.18.1.1115-1127

[12] A. Suthatho, Low-density all-cellulose composites made from cotton textile waste with promising thermal insulation and acoustic absorption properties. Acs Applied Polymer Materials, 6 (**2023**) 1, 390–397. doi:10.1021/acsapm.3c02076

[13] S. Tanpichai, F. Phoothong, A. Boonmahitthisud, Superabsorbent cellulose-based hydrogels cross-liked with borax. Scientific Reports, 12 (**2022**) 1. doi:10.1038/s41598-022-12688-2

[14] S. Aswathy, U. Narendrakumar, I. ManjubalaPhysicochemical properties of cellulose-based hydrogel for biomedical applications. Polymers, 14 (**2022**) 21, 4669. doi:10.3390/polym14214669

[15] P. Basu, U. Narendrakumar, R. Arunachalam, S. Devi, I. Manjubala, Characterization and evaluation of carboxymethyl cellulose-based films for healing of full-thickness wounds in normal and diabetic rats. Acs Omega, 3 (**2018**) 10, 12622–12632. doi:10.1021/acsomega.8b02015

[16] P. Cuadro, T. Belt, K. Kontturi, M. Reza, E. Kontturi, T. Vuorinen, … M. Hughes, Cross-linking of cellulose and poly(ethylene glycol) with citric acid. Reactive and Functional Polymers, 90 (**2015**), 21–24. doi:10.1016/j.reactfunctpolym.2015.03.007

[17] D. Das, P. Prakash, P. Rout, S. Bhaladhare, Synthesis and characterization of superabsorbent cellulose-based hydrogel for agriculture application. Starch – Stärke, 73 (**2020**) 1–2. doi:10.1002/star.201900284

[18] G. Frühauf, L. Beltrami, E. Francisquetti, C. Granada, A. Zattera, A. Catto, … C. Borsoi, Fungicidal potential of polymeric hydrogels based on carboxymethylcellulose and yerba mate residues with the incorporation of garlic oil. Starch - Stärke, 75 (**2022**) 3–4. doi:10.1002/star.202200182

[19] M. Hassan, N. Tucker, M. Guen, Thermal, mechanical and viscoelastic properties of citric acid-crosslinked starch/cellulose composite foams. Carbohydrate Polymers, 230 (**2020**), 115675. doi:10.1016/j.carbpol.2019.115675

[20] G. Isopencu, I. Deleanu, C. Busuioc, O. Oprea, V. Surdu, M. Bacalum, … A. Stoica-Guzun, Bacterial cellulose – carboxymethylcellulose composite loaded with turmeric extract for antimicrobial wound dressing applications. International Journal of Molecular Sciences, 24 (**2023**) 2, 1719. doi:10.3390/ijms24021719

[21] G. Lima, A. Souza, D. Rosa, Nanocellulose as reinforcement in carboxymethylcellulose superabsorbent nanocomposite hydrogels. Macromolecular Symposia, 394 (**2020**) 1. doi:10.1002/masy.202000126

[22] K. Mali, S. Dhawale, R. Dias, N. Dhane, V. Ghorpade, Citric acid crosslinked carboxymethyl cellulose-based composite hydrogel films for drug delivery. Indian Journal of Pharmaceutical Sciences, 80 (**2018**) 4. doi:10.4172/pharmaceutical-sciences.1000405

[23] A. Mandal, D. Chakrabarty, Studies on mechanical, thermal, and barrier properties of carboxymethyl cellulose film highly filled with nanocellulose. Journal of Thermoplastic Composite Materials, 32 (**2018**) 7, 995–1014. doi:10.1177/0892705718772868

[24] N. Nazri, Y. Kumar, M. Ramlan, M. Kassim, M. Hossain, N. Kaus, Physico-mechanical study of cmc/bfo/popd nanocomposite films reinforced with cellulose nanocrystals (cncmcc) for effective photocatalytic removal of methyl orange. Journal of Composites Science, 5 (**2021**). 6, 142. doi:10.3390/jcs5060142

[25] G. Priya, B. Madhan, U. Narendrakumar, R. Kumar, I. Manjubala, in vitro and in vivo evaluation of carboxymethyl cellulose scaffolds for bone tissue engineering applications. Acs Omega, 6 (**2021**) 2, 1246–1253. doi:10.1021/acsomega.0c04551

[26] N. Alqahtani, T. Alnemr, F. Shulaybi, H. Mohamed, M. Gouda, Carboxymethyl-cellulose-containing ag nanoparticles as an electrochemical working electrode for fast hydroxymethyl-furfural sensing in date molasses. Polymers, 15 (**2022**) 1, 79. doi:10.3390/polym15010079

[27] R. Badry, M. El-Nahass, N. Nada, H. Elhaes, M. Ibrahim, Structural and uv-blocking properties of carboxymethyl cellulose sodium/cuo nanocomposite films. Scientific Reports, 13 (**2023**) 1. doi:10.1038/s41598-023-28032-1

[28] R. Nuisin, T. Siripongpreda, S. Watcharamul, K. Siralertmukul, S. Kiatkamjornwong, Facile syntheses of physically crosslinked carboxymethyl cellulose hydrogels and nanocomposite hydrogels for enhancing water absorbency and adsorption of sappan wood dye. Chemistryselect, 7 (**2022**) 10. doi:10.1002/slct.202104598

[29] H. Wang, J. Wu, B. Huang, Q. Lu, One-pot synthesis of upy-functionalized nanocellulose under mechanochemical synergy for high-performance epoxy nanocomposites. Polymers, 14 (**2022**) 12, 2428. doi:10.3390/polym14122428

[30] E. Brown, D. Hu, N. Lail, X. Zhang, Potential of nanocrystalline cellulose–fibrin nanocomposites for artificial vascular graft applications. Biomacromolecules, 14 (**2013**) 4, 1063–1071. doi:10.1021/bm3019467

[31] M. Bulota, A. Vesterinen, M. Hughes, J. Seppälä, Mechanical behavior, structure, and reinforcement processes of tempo-oxidized cellulose reinforced poly(lactic) acid. Polymer Composites, 34 (**2012**) 2, 173–179. doi:10.1002/pc.22390

[32] E. Indarti, R. Rohaizu, M. Husin, W. Daud, Polylactic acid bionanocomposites filled with nanocrystalline cellulose from tempo-oxidized oil palm lignocellulosic biomass. Bioresources, 11 (**2016**) 4, 8615–8626. doi:10.15376/biores.11.4.8615-8626

[33] S. Pashaei, S. Mohammadi-Aghdam, S. Hosseinzadeh, Physico-mechanical, dynamic mechanical, and morphological properties of polyurethane/ncc/agnp nanocomposites and their application in removal of heavy metals from wastewater. Polymer Composites, 40 (**2019**) 10, 4004-4012. doi:10.1002/pc.25261

[34] I. Sacui, R. Nieuwendaal, D. Burnett, S. Stranick, M. Jorfi, C. Weder, … J. Gilman, Comparison of the properties of cellulose nanocrystals and cellulose nanofibrils isolated from bacteria, tunicate, and wood processed using acid, enzymatic, mechanical, and oxidative methods. Acs Applied Materials & Interfaces, 6 (**2014**) 9, 6127–6138. doi:10.1021/am500359f

[35] H. Tazeen, N. Varadharaju, M. Kannan, Preparation and characterization of nanocrystalline cellulose for development of nanocomposite films. Asian Journal of Chemistry, 29 (**2017**) 12, 2687–2691. doi:10.14233/ajchem.2017.20804

[36] J. Yu, F. Zhang, Y. Xu, J. Qu, G. Zhang, Y. Lv, … Y. Xia, Effect of nanocrystalline cellulose on mechanical, thermal, and barrier properties of polylactic acid blown composite film. Polymers for Advanced Technologies, 34 (**2023**) 5, 1662–1670. doi:10.1002/pat.6000

[37] T. Aravind, M. Ashraf, A. Rajesh, N. Ahalya, M. Rawat, B. Uma, … S. Sida, Study of progress on nanocrystalline cellulose and natural fiber reinforcement biocomposites. Journal of Nanomaterials, (**2022**) 1. doi:10.1155/2022/6519480

[38] S. Borysiak, A. Grząbka-Zasadzińska, Influence of the polymorphism of cellulose on the formation of nanocrystals and their application in chitosan/nanocellulose composites. Journal of Applied Polymer Science, 133 (**2015**) 3. doi:10.1002/app.42864

[39] A. Grząbka-Zasadzińska, W. Smułek, E. Kaczorek, S. Borysiak, Chitosan biocomposites with enzymatically produced nanocrystalline cellulose. Polymer Composites, 39 (**2017**) S1. doi:10.1002/pc.24552

[40] Y. Habibi, L. Lucia, O. Rojas, Cellulose nanocrystals: chemistry, self-assembly, and applications. Chemical Reviews, 110 (**2010**) 6, 3479–3500. doi:10.1021/cr900339w

[41] M. Ioelovich, Study of cellulose interaction with concentrated solutions of sulfuric acid. Isrn Chemical Engineering, (**2012**), 1–7. doi:10.5402/2012/428974

[42] M. Muhamin, P. Purwanto, W. Astuti, K. Triyana, Nanocrystalline cellulose studied with a conventional sem. (**2014**). doi:10.2991/icp-14.2014.3

[43] A. Rani, S. Monga, M. Bansal, A. Sharma, Bionanocomposites reinforced with cellulose nanofibers derived from sugarcane bagasse. Polymer Composites, 39 (**2016**) S1. doi:10.1002/pc.24112

[44] G. Siqueira, J. Bras, A. Dufresne, Cellulosic bionanocomposites: a review of preparation, properties and applications. Polymers, 2 (**2010**) 4, 728–765. doi:10.3390/polym2040728

[45] X. Zheng, W. Sun, A. Li, B. Wang, R. Jiang, Z. Song, … Z. Li, Graphene oxide and polyethyleneimine cooperative construct ionic imprinted cellulose nanocrystals aerogel for selective adsorption of dy(iii). (**2021**). doi:10.21203/rs.3.rs-586534/v2

[46] A. E. Oral, S. Aytas, S. Yusan, S. Sert, C. Gok, O. Elmastas Gultekin Preparation and characterization of a graphene-based magnetic nanocomposite for the adsorption of lanthanum ions from aqueous solution. Anal Lett 53 (**2020**) 11, 1812–1833. doi:10.1080/00032719.2020.1719128

[47] X. Jaramillo-Fierro, S. Gaona, E. Valarezo, La3+'s effect on the surface (101) of anatase for methylene blue dye removal, a dft study. Molecules, 27 (**2022**) 19, 6370. doi:10.3390/molecules27196370

[48] W. Sung, D. Vaknin, D. Kim, Different adsorption behavior of rare earth and metallic ion complexes on langmuir monolayers probed by sum-frequency generation spectroscopy. Journal of the Optical Society of Korea, 17 (**2013**) 1, 10–15. doi:10.3807/josk.2013.17.1.010

[49] N. Nunotani, M. Misran, M. Inada, T. Uchiyama, Y. Uchimoto, N. Imanaka, Structural environment of chloride ion-conducting solids based on lanthanum oxychloride. Journal of the American Ceramic Society, 103 (**2019**) 1, 297–-303. doi:10.1111/jace.16727